First examples of polynuclear lanthanide diethylene glycol based coordination clusters

Article (Accepted Version)

EurJIC
European Journal of Inorganic Chemistry

A Journal of ChemPubSoc Europe

Accepted Article

Title: First examples of polynuclear lanthanide diethylene glycol based coordination clusters

Authors: Guo Peng, Ying-Ying Zhang, Zhao-Yang Li, and George E Kostakis

To be cited as: *Eur. J. Inorg. Chem.* 10.1002/ejic.201700168

Link to VoR: http://dx.doi.org/10.1002/ejic.201700168

WILEY-VCH

First examples of polynuclear lanthanide diethylene glycol based coordination clusters

Guo Peng,*[a] Ying-Ying Zhang,[a] Zhao-Yang Li[b] and George E. Kostakis[c]

Abstract: Five lanthanide coordination clusters (CCs) $[Ln_7(\mu_3\text{-}OH)_4(deg)_2(Hdeg)_2(ben)_{11}]\cdot xCH_3CN$ [Ln=Eu (**1**), Gd (**2**), Tb (**3**), Dy (**4**), Ho (**5**); H_2deg=diethylene glycol, Hben=benzoic acid, x=7 for **1**-**4** and 6 for **5**] with diethylene glycol and benzoic acid as ligands have been prepared and structurally characterized. All CCs consist of a heptanuclear lanthanide core with a scarce tip-sharing double-butterfly topology. Magnetic measurements revealed that CC **4** exhibits slow magnetic relaxation with an energy barrier of about 6K, whereas CC **3** shows outstanding magnetocaloric effect with entropy change of 34.6 J Kg^{-1} K^{-1} at 2K and ΔH=7T. The photoluminescent properties of CCs **1**, **3** and **4** were also investigated, displaying intense characteristic emission spectra of Eu^{III}, Tb^{III} and Dy^{III} ions.

Introduction

Nano-size lanthanide coordination clusters (CCs) have been widely explored in the recent past due to their fascinating single molecule magnet (SMM),[1] magnetic cooler,[2] and luminescent properties.[3] SMMs show slow relaxation or/and hysteresis below a certain temperature (called blocking temperature), and thus can be considered as good candidates for high density information storage, quantum computing and spintronic devices.[4] The behavior of SMMs depends on the spin ground state and anisotropy. The heavy lanthanide ions, such as Tb^{III}, Dy^{III}, Ho^{III}, carry significant spin and present high anisotropy deriving from strong spin-orbital coupling. Therefore, CCs with assembly of such heavy lanthanide ions could show remarkable ability to behavior as SMM. On the contrary, CCs with Gd^{III} ions, where Gd^{III} ion is isotropic and has a large spin, can exhibit large magnetocaloric effect (MCE), which can act as eco-friendly coolant for liquid helium temperature cooling.[2] Besides the intriguing magnetic properties, lanthanide CCs have also displayed strong, narrow and long-lived emissions from visible to near-infrared region arising from internal f-f transitions, which results in their diverse applications as electroluminescent devices and bio-sensors.[5]

To stabilize a lanthanide CC with interesting magnetic or/and luminescent properties, the selection of appropriate organic ligand which can bridge lanthanide ions for magnetic information and energy transfer is crucial. Several types of ligands, such as Schiff-base,[6] diketone,[7] carboxylic acid,[8] ethanolamine[9] and calixarene,[10] have been employed to construct lanthanide CCs and their nuclearity vary from 2 to 104.[1-2, 6-12] Lanthanides are hard Lewis acids and thus have high affinity to coordinate with oxygen donors.

In this work, we decided to use a mixed ligand synthetic strategy for the synthesis of new polynuclear lanthanide CCs incorporating diethylene glycol (H_2deg) and benzoic acid (Hben). The reason for the selection of this system is manifold. A) Both organic molecules bear only oxygen atoms as donors. B) H_2deg was used in lanthanide coordination chemistry for the first time almost three decades ago, however, the nuclearity of all the resulting products was limited to one or two.[13] C) It has been established that benzoic acid not only can give additional bridging between cations, leading to larger CCs, but also provide various pathways for magnetic interactions and energy transfer (antenna effect).[14] As a result, a series of heptanuclear lanthanide CCs, formulated $[Ln_7(\mu_3\text{-}OH)_4(deg)_2(Hdeg)_2(ben)_{11}]\cdot xCH_3CN$ [Ln=Eu (**1**), Gd (**2**), Tb (**3**), Dy (**4**), Ho (**5**); x=7 for **1**-**4** and 6 for **5**] with scarce tip-sharing double-butterfly topology were isolated, and their SMM, magnetic cooler and emissions behavior were studied.

Results and Discussion

Synthetic aspects

The reaction of H_2deg, Hben, $Ln(NO_3)_3\cdot 6H_2O$ and Et_3N (molar ratio 10:1:0.5:2) in CH_3CN under aerobic condition produced five CCs, formulated $[Ln_7(\mu_3\text{-}OH)_4(deg)_2(Hdeg)_2(ben)_{11}]\cdot xCH_3CN$ where Ln=Eu (**1**), Gd (**2**), Tb (**3**), Dy (**4**), Ho (**5**); x=7 for **1**-**4** and 6 for **5**. Experiments with different ratio (1:1:0.5:2) or changing the raw material from $Ln(NO_3)_3\cdot 6H_2O$ to $LnCl_3\cdot 6H_2O$ gave the same products, in lower yields, as it was confirmed by IR and PXRD studies. The crystals of **1**-**5** lose the lattice solvent CH_3CN and absorb water quickly in the air after filtration, which has been verified by elemental analyses and IR spectra (Figure S1). The PXRD patterns of **1**-**5** deviate from the simulated one due to the replacement of lattice CH_3CN by water. All the experimental PXRD patterns are similar, confirming the isomorphous nature of **1**-**5** (Figure S2).

Structural analysis

Single crystal X-ray diffraction analyses show that all five CCs are isoskeletal and crystallize in triclinic space group *P*-1 with *Z*=2. Therefore, only the structure of **4** is described here in detail. The asymmetric unit of **4** consists of a neutral

[a] Guo Peng, Ying-Ying Zhang
Herbert Gleiter Institute of Nanoscience, Nanjing University of Science and Technology, 210094 Nanjing, P. R. China.
E-mail: guopeng@njust.edu.cn
[b] Zhao-Yang Li
Department of Chemistry and Graduate School of Science, Tohoku University, 6-3 Aramaki-Aza-Aoba, Aoba-ku, 980-8578, Sendai, Japan
[c] Department of Chemistry, School of Life Sciences, University of Sussex, Brighton, BN1 9QJ, UK

Supporting information for this article is given via a link at the end of the document.((Please delete this text if not appropriate))

heptanuclear $[Dy_7(\mu_3\text{-}OH)_4(deg)_2(Hdeg)_2(ben)_{11}]$ CC and seven acetonitrile molecules (Figure 1a). The heptanuclear core can be described as two $Dy_4(\mu_3\text{-}OH)O_4$ "butterflies" sharing the wing-tip position (Dy4) (Figure 1b). All seven Dy^{III} ions are eight coordinate and their coordination geometries derived from Shape 2.1 program[15] can be divided into three types: Dy1, Dy2, Dy6 and Dy7 possess a triangular dodecahedral configuration, whereas Dy3 and Dy5 with biaugmented trigonal prismatic and Dy4 with square antiprismatic geometries (Table S1). The periphery of the core is surrounded by four diethylene glycol ligands and eleven benzoate groups. Two, single deprotonated, diethylene glycol ligands chelate to one Dy and bridge to other Dy ions with a μ_2: η^2 η^1 η^1 mode (Scheme 1a), whereas the other two, double deprotonated, diethylene glycol ligands chelate to one Dy and bridge to three other Dy ions in a μ_3: η^2 η^1 η^3 coordination fashion (Scheme 1b). To the best of our knowledge, these two coordination modes have never been observed in the literature before. The eleven benzoate groups adopt three different coordination modes, namely, μ_1: η^1 η^1, μ_2: η^1 η^1 and μ_2: η^1 η^2, respectively (Scheme 1c-e). The Dy-O bond lengths vary from 2.256(6) to 2.633(5) Å and the nearest intramolecular Dy···Dy separations are in the range of 3.6306(5) -3.9041(5) Å.

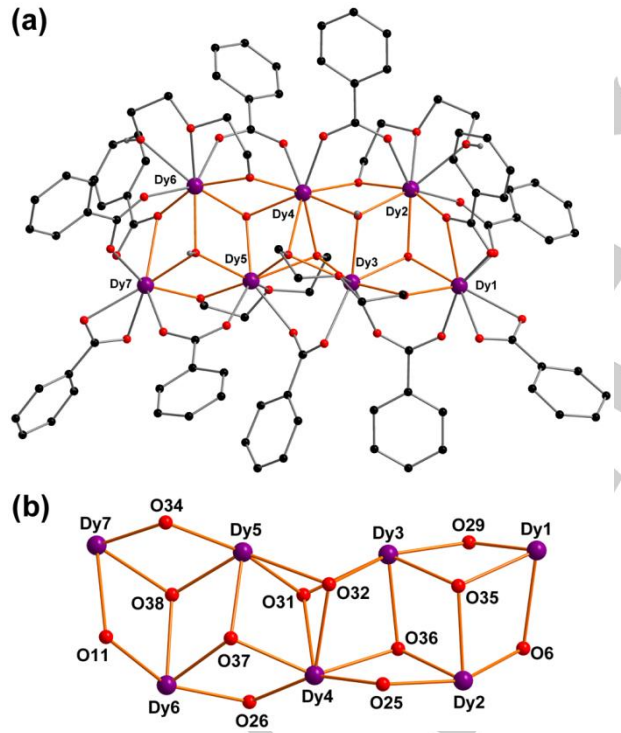

Figure 1. (a) Molecular structure of CC **4** and (b) its Dy_7 core. Dy is shown in violet, O in red and C in black. H atoms and solvent molecules are omitted for clarity.

Topological aspects

Although several heptanuclear lanthanide CCs with different topologies[12], such as discs,[12a] trigonal prism,[12b-d] capped octahedron,[12e-f] dicubane,[12g-i] cyclic shape,[12j-k] have been documented before, the tip-sharing double-butterfly topology is rarely observed in the literature. Recently, a serials of heptanuclear lanthanide CCs $(NHEt_3)[Ln_7(OH)_2(saph)_{10}(Me_2CO)_2]$ [Ln=Gd (**6**), Tb (**7**), Dy (**8**), $saphH_2$= N-salicylidene-o-aminophenol] with similar topology to CCs **1**-**5** has been reported by Stamatatos *et al*.[12l] The organic ligand ($saphH_2$) (Scheme S1a) used to yield CCs **6**-**8** offers similar coordination pockets with H_2deg (Scheme S1b). However, a comparison with CCs **6**-**8**, the heptanuclear CCs **1**-**5** have more OH^- and benzoate bridging units, which are important for transferring magnetic interactions. Moreover, CCs **1**-**5** are neutral and **6**-**8** are negative charged. Interestingly, an automatic graphical search of all polynuclear CCs (3d, 4f, 3d-4f, 4d) shows that this topology (**2,3,4M7-2**) (Figure S3) has been seen only in 4f chemistry.[16]

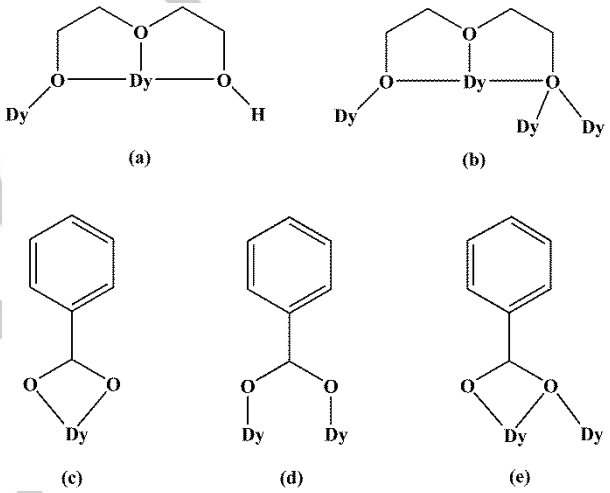

Scheme 1. Coordination modes of diethylene glycol and benzoate in CC **4**.

Magnetic studies

Static magnetic susceptibility measurements were performed on polycrystalline samples of **2**-**5** in the temperature range of 2-300K under an applied direct-current (dc) field of 1000Oe, and the magnetic data based on these measurements are summarized in Table 1. The room temperature χT values of **2-5** are close to the expected values for seven isolated Ln^{III} ions (Table 1). On cooling, the χT product of **2** slightly decreases with decreasing temperature to 50K and then sharply decreases to 24.75 cm^3 K mol^{-1} at 2K (Figure 2), indicating the presence of antiferromagnetic interactions between Gd^{III} ions. Fitting the χ^{-1} versus T curve of **2** in the range of 50-300K by the Curie–Weiss law results in θ=-2.08 and C=55.31 cm^3 K mol^{-1} (Figure S4). The negative Weiss constant further confirms the overall antiferromagnetic coupling in this system. In the case of **3** and **5**, the χT values decrease with cooling over the whole temperature range, which is probably due to a combination of intramolecular antiferromagnetic interactions and thermal depopulation of the Stark sublevels of Tb^{III} or Ho^{III} ions (Figure 2). For **4**, the χT product gradually decreases to a minimum of 87.60 cm^3 K mol^{-1}

Table 1. Direct current (dc) magnetic data for CCs **2**-**5**.

CCs	Ground state of Ln^{III}	Expected χT at 300K (cm^3Kmol^{-1})	Measured χT at 300K (cm^3Kmol^{-1})	Saturation magnetization (Nβ)	Measured magnetization at 2K and 70KOe (Nβ)
2-Gd_7	$^8S_{7/2}$	55.16	54.89	49	46.69
3-Tb_7	$^7F_6$	82.74	82.23	63	32.98
4-Dy_7	$^6H_{15/2}$	99.19	98.13	70	38.11
5-Ho_7	$^5I_8$	98.49	95.13	70	34.64

at 11K and then abruptly increases to 93.89 cm^3 K mol^{-1} at 2K (Figure 2). Such behavior suggests that the presence of ferromagnetic interactions between Dy^{III} ions below 11K, and the decrease above 11K is likely due to the thermal depopulation of the Stark sublevels of Dy^{III} ion. The static magnetic behaviors of **2**, **3** and **5** are similar with other Gd_7, Tb_7 and Ho_7 CCs, respectively, but that of **4** is different from other Dy_7 systems reported in the literature.[12] Ferromagnetic couplings at low temperature were observed in the Dy_7 CC reported herein, but such behavior was not detected in other Dy_7 systems.[12]

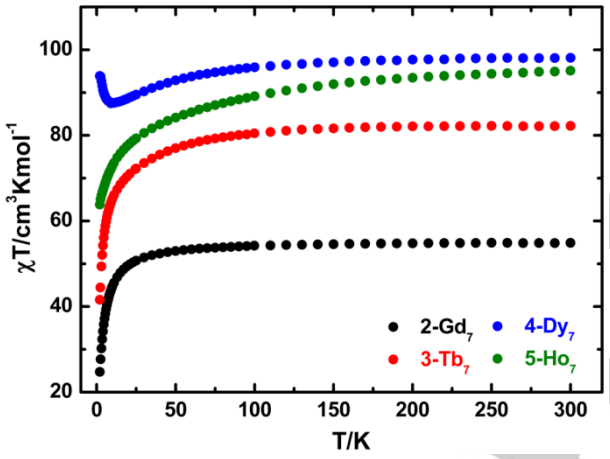

Figure 2. Temperature dependence of the χT products for CCs **2**-**5**.

The magnetization of **2** almost reaches saturation at 2K and 70KOe (Table 1 and Figure S5a), indicating the absence of any significant anisotropy in this system. For **3**-**5**, their magnetizations below 5K increase with rising applied field and without reach saturation even up to 70KOe (Table 1 and Figure S5b-d). The lack of saturation at low temperature and high magnetic field indicates the existence of anisotropy and/or low-lying excited states in these systems. This conclusion is further proved by M versus HT^{-1} plots below 5K, which are non-superposed on a master curve (Figure S6), as expected for systems with anisotropy and/or low-lying excited states.

In view of the magnetic anisotropy possessing by **3**-**5**, the altering-current (ac) susceptibility measurements were conducted to probe the magnetic dynamic of these systems. No ac signals were observed for **3** and **5**. In the case of **4**, the out-of-phase ac susceptibilities show clear frequency dependent, but no maxima were detected above 2K (Figure 3 and Figure S7), suggesting fast relaxation of the magnetization. In order to slow down the relaxation, further ac susceptibility measurements were performed under different external field at 2K. The out-of-phase ac components under different dc fields show little change (Figure S8), indicating the relaxation dynamic of this system is not influence by quantum effects at least above 2K.[17] Considering a single relaxation process, the energy barrier (E_a) and pre-exponential factor (τ_0) of **4** can be roughly estimated by equation: $\ln(\chi''/\chi') = \ln(\omega\tau_0) + E_a/k_B$.[18] The least-squares fits of the ac data gave an energy barrier of ~6.0K and a pre-exponential factor of ~2.35×10^{-6}s (Figure 3 inset), which is consistent with the expected values (τ_0=10^{-6}-10^{-11} s) for SMMs.[1]

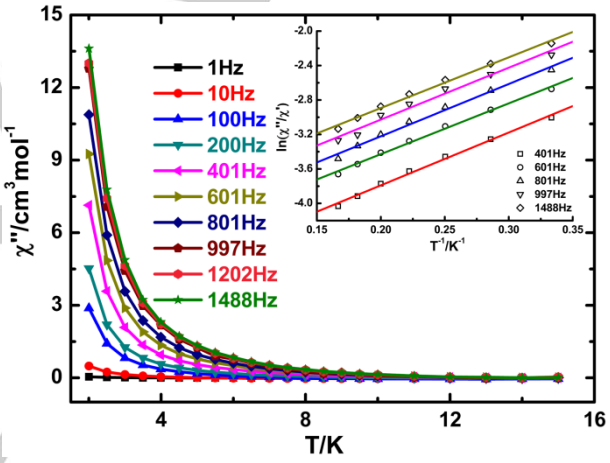

Figure 3. Temperature dependence of out-of-phase ac magnetic susceptibility signals under zero dc field for CC **4**. (Inset) ln(χ''/χ') versus T^{-1} plots at different frequencies; The lines are the best-fit curves.

Due to the large spin of Gd^{III} and the absent of magnetic anisotropy, the magnetic entropy change (-ΔS_m) of **2** was investigated to assess the magnetic caloric effect (MCE). The -ΔS_m can be extracted from magnetization data (Figure S9) by using Maxwell equation: $\Delta S_m(T) = \int_0^H [\partial M(T,H)/\partial T]_H dH$. As shown in Figure 4, the maximum of -ΔS_m for **2** is 34.6 J Kg^{-1} K^{-1} at 2K and ΔH=7T, which is lower than the expected value of 39.4 J Kg^{-1} K^{-1} calculating by $nR[ln(2S+1)]/M_w$ with S=7/2 for seven isolated Gd^{III} ions, but its value is still comparable to that of other Gd-based CCs, such as Gd_5 (34 J Kg^{-1} K^{-1} at 3K and ΔH=7T), Gd_8 (32.3 J Kg^{-1} K^{-1} at 3K and ΔH=7T), Gd_{10} (31.2 J Kg^{-1} K^{-1} at 3K and ΔH=7T) and Gd_{12} (35.3 J Kg^{-1} K^{-1} at 3K and ΔH=7T).[19] To the best of our knowledge, the experimental value of **2** is higher than that of other Gd_7 CCs so far discovered.[12a, b, g, h]

Potoluminescent properties

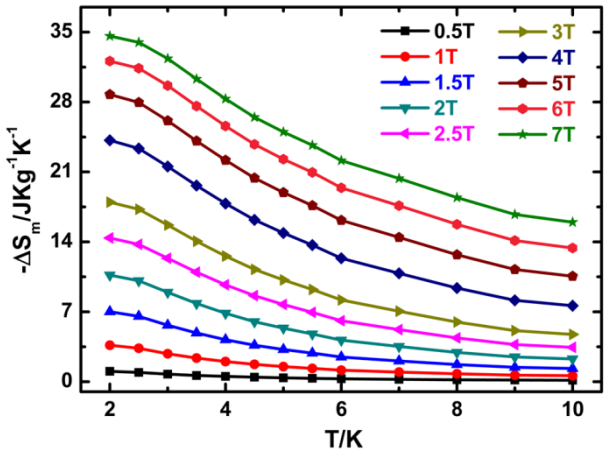

Figure 4. Temperature dependence of the entropy change under different magnetic field obtained from magnetization data of CC **2**.

In light of the excellence luminescent properties of Eu^{III}, Tb^{III} and Dy^{III} ions, the potoluminescent spectra of CCs **1**, **3** and **4** were recorded in solid state at room temperature. Under excitation at 393nm (Figure S10a), CC **1** produces strong red emission and displays characteristic peaks at 579, 592, 617, 652 and 699nm originating from the $^5D_0 \rightarrow {}^7F_J$ (J=0→4) transition of Eu^{III} ion (Figure 5). The presence of the symmetry-forbidden emission $^5D_0 \rightarrow {}^7F_0$ at 579nm suggests that the coordination environment of Eu^{III} ions possess low symmetry.[20] The $^5D_0 \rightarrow {}^7F_1$ emission at 592nm belongs to magnetic dipole character and its intensity is almost not influenced by coordination environment.[20]

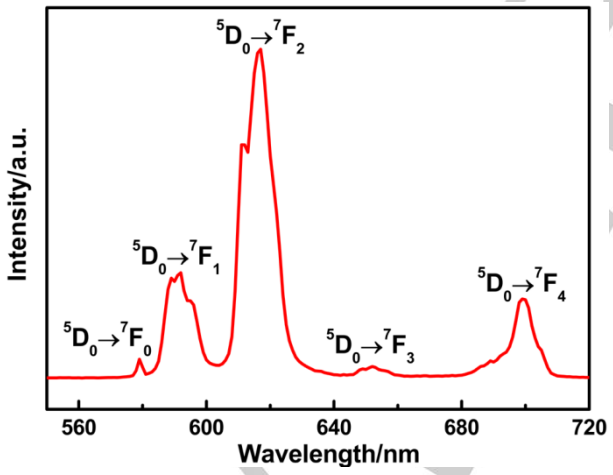

Figure 5. Solid-state emission spectra of CC **1** at room temperature.

The electric dipole $^5D_0 \rightarrow {}^7F_2$ transition at 617nm is much stronger than $^5D_0 \rightarrow {}^7F_1$ transition at 592nm, indicating the absence of inversion symmetry at Eu^{III} centers,[3a, 20] which is consistent with the results from single crystal diffraction. CC **3** emits green light under excitation at 369nm (Figure S10b) and yields a typical Tb^{III} emission spectrum (Figure 6). The emission bands at 491, 545,

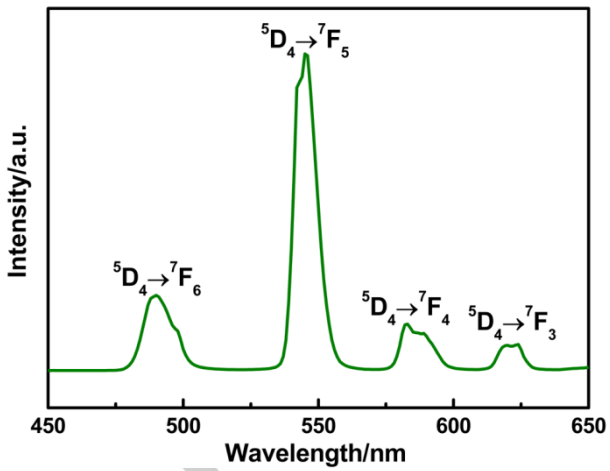

Figure 6. Solid-state emission spectra of CC **3** at room temperature.

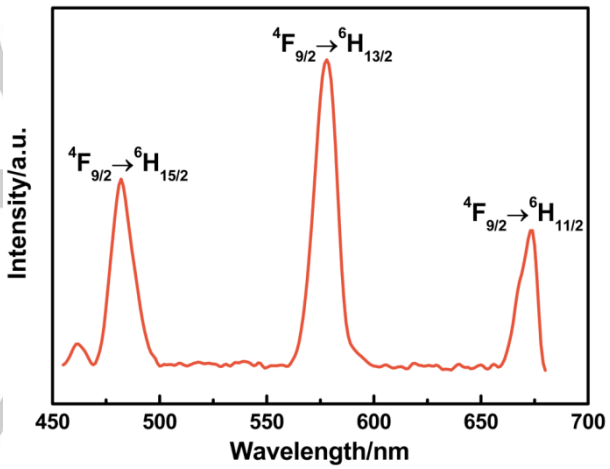

Figure 7. Solid-state emission spectra of CC **4** at room temperature.

583, 620nm can be attribute to the $^5D_4 \rightarrow {}^7F_J$ (J=6→3) transition of Tb^{III} ion. The spectrum is dominated by the hypersensitive $^5D_4 \rightarrow {}^7F_5$ transition, which is responsible for the green emission. As shown in Figure 7, the spectrum of **4** exhibits three emission peaks at 482, 578 and 673nm under excitation at 350nm (Figure S10c), which correspond to the transition from the $^4F_{9/2}$ excited state to ^6H_J (J=15/2, 13/2 and 11/2). The most intensive emission at 578nm belongs to the $^4F_{9/2} \rightarrow {}^6H_{13/2}$ transition of Dy^{III} center, which is responsible for the yellow emission. The intensity of yellow emission ($^4F_{9/2} \rightarrow {}^6H_{13/2}$) is higher than that of blue emission ($^4F_{9/2} \rightarrow {}^6H_{15/2}$) in the spectrum of **4**. This observation suggests that Dy^{III} ions are located at low symmetric coordination environment,[21] which is in agreement with the crystallographic results. All three CCs display characteristic emission spectra of corresponding lanthanide ions. It means that the ligands can sensitize the photoluminescence of lanthanide centers effectively. The luminescence decay curves of CCs **1**, **3** and **4** were investigated by monitoring the emissions at 617, 545

and 578 nm in solid state at room temperature (Figure S11). The average lifetime values obtained for CCs **1**, **3** and **4** are 580.4, 1441.8 and 6.8μs respectively, which are comparable to that of other Eu^{III}, Tb^{III} and Dy^{III} complexes.[3c, 14b, 22]

Conclusions

The first examples of polynuclear CCs constructed from H_2deg are reported in this study. Five heptanuclear lanthanide CCs with scarce tip-sharing double-butterfly topology have been obtained by using a mixed ligand synthetic protocol incorporating diethylene glycol and benzoic acid as ligands. The present synthetic strategy yields CC **4** that shows slow magnetic relaxation with an energy barrier of about 6K, and **3** that possesses outstanding MCE with entropy change of 34.6 J Kg^{-1} K^{-1} at 2K and Δ*H*=7T, which is highest among the already reported Gd_7 CCs.[12a, b, g, h] Additionally, CCs **1**, **3** and **4** display the characteristic emissions of corresponding lanthanide ions at room temperature. This work illustrates that the proposed mixed oxygen-donor ligand synthetic strategy is an effective synthetic tool to construct high nuclearity CCs with fascinating magnetic and luminescent properties. Ongoing investigations for the synthesis of other derivatives are in progress in our laboratory.

Experimental Section

Synthetic procedures

All the materials and reagents were obtained from commercial sources, and were used as received without further purification. All reactions were carried out under aerobic condition. Similar procedure was employed to prepare CCs **1**-**5** and hence only the synthesis of CC **1** is described here in detail.

$[Eu_7(\mu_3\text{-}OH)_4(deg)_2(Hdeg)_2(ben)_{11}]\cdot 7CH_3CN$ (1) A mixture of diethylene glycol (1.068g, 10mmol), benzoic acid (0.122g, 1mmol) and $Eu(NO_3)_3\cdot 6H_2O$ (0.223g, 0.5mmol) was dissolved in CH_3CN (20mL). The mixture was stirred for 30min at 55ºC, and then triethylamine (0.28mL, 2mmol) was added. The resulting mixture was stirred for another 3h at 55 ºC and then filtered when the solution was cooled. Slow evaporation of the filtrate at room temperature gave colorless crystals after several days. Yield: 47mg (22% based on Eu). Calc. (%) for $C_{93}H_{93}Eu_7O_{38}\cdot 0.5CH_3CN\cdot 8H_2O$: C 37.05, H 3.66, N 0.23; found: C 37.03, H 3.51, N 0.21. Selected IR data (cm^{-1}): 3420(br), 3064(w), 2922(w), 2869(w), 2259(w), 1597(m), 1548(m), 1405(s), 1176(w), 1089(w), 1049(w), 1025(w), 919(w), 852(w), 719(m), 689(w), 575(w).

$[Gd_7(\mu_3\text{-}OH)_4(deg)_2(Hdeg)_2(ben)_{11}]\cdot 7CH_3CN$ (2). Yield: 80mg (36% based on Gd). Calc. (%) for $C_{93}H_{93}Gd_7O_{38}\cdot 0.7CH_3CN\cdot 7H_2O$: C 36.88, H 3.58, N 0.32; found: C 36.66, H 3.30, N 0.34. Selected IR data (cm^{-1}): 3420(br), 3064(w), 2924(w), 2870(w), 1597(m), 1548(m), 1405(s), 1177(w), 1090(w), 1050(w), 1025(w), 919(w), 856(w), 718(m), 689(w), 577(w).

$[Tb_7(\mu_3\text{-}OH)_4(deg)_2(Hdeg)_2(ben)_{11}]\cdot 7CH_3CN$ (3). Yield: 146mg (66%, based on Tb). Calc. (%) for $C_{93}H_{93}Tb_7O_{38}\cdot 0.9CH_3CN\cdot 7H_2O$: C 36.80, H 3.57, N 0.41; found: C 36.70, H 3.31, N 0.40. Selected IR data (cm^{-1}): 3424(br), 3062(w), 2927(w), 2866(w), 2259(w), 1597(m), 1548(m), 1407(s), 1177(w), 1090(w), 1051(w), 1025(w), 921(w), 857(w), 719(m), 689(w), 580(w).

$[Dy_7(\mu_3\text{-}OH)_4(deg)_2(Hdeg)_2(ben)_{11}]\cdot 7CH_3CN$ (4). Yield: 153mg (69%, based on Dy). Calc. (%) for $C_{93}H_{93}Dy_7O_{38}\cdot CH_3CN\cdot 6.5H_2O$: C 36.64, H 3.53, N 0.45; found: C 36.44, H 3.24, N 0.47. Selected IR data (cm^{-1}): 3424(br), 3065(w), 2928(w), 2870(w), 2261(w), 1598(m), 1550(m), 1406(s), 1176(w), 1091(w), 1051(w), 1025(w), 922(w), 857(w), 719(m), 689(w), 582(w).

$[Ho_7(\mu_3\text{-}OH)_4(deg)_2(Hdeg)_2(ben)_{11}]\cdot 6CH_3CN$ (5). Yield: 173mg (77%, based on Ho). Calc. (%) for $C_{93}H_{93}Ho_7O_{38}\cdot CH_3CN\cdot 6.5H_2O$: C 36.44, H 3.51, N 0.45; found: C 36.15, H 3.21, N 0.46. Selected IR data (cm^{-1}): 3432(br), 3065(w), 2930(w), 2870(w), 2259(w), 1598(m), 1552(m), 1409(s), 1176(w), 1092(w), 1051(w), 1025(w), 924(w), 858(w), 719(m), 689(w), 584(w).

Physical measurements

Elemental analyses (C, H and N) were performed on an Elementar Vario EL elemental analyser. Fourier transform IR spectra were measured on a Nicolet IS10 Spectrum with samples prepared as KBr discs. Powder X-Ray diffraction patterns for all complexes were measured at room temperature using a Bruker D8 ADVANCE X-ray diffractometer. Magnetic measurements were conducted on a Quantum Design MPMS-XL SQUID magnetometer or a Quantum Design PPMS DynaCool-9 magnetometer. The magnetic data were processed by using formula weight from elemental analysis. The magnetic data were corrected for diamagnetic contribution by using Pascal's constants. The luminescent spectra were recorded on a Jobin Yvon FL3-TCSPC fluorescence spectrometer. The lifetimes of CCs **1**, **3** and **4** were explored by an Edinburgh FLS-920 fluorescence spectrometer. The decay curves of CCs **1**, **3** and **4** were fitted by a double exponential function, $I = A + B_1\exp(-t/\tau_1) + B_2\exp(-t/\tau_2)$ and the average lifetimes (*τ*) were calculated by equation, $\tau = (B_1\tau_1^2 + B_2\tau_2^2)/(B_1\tau_1 + B_2\tau_2)$.[23]

Single crystal X-ray diffraction

The data of **1**-**5** were collected on a Bruker SMART APEX II diffractometer at 173(2)K using graphite-monochromated Mo-Kα radiation. All structures were solved by direct methods and refined by full-matrix least squares analysis on F^2, using the SHELXTL package.[24] Ordered non-H atoms were refined anisotropically, H-atoms were placed in calculated positions and refined using a riding model. The contributions from severely disordered solvent molecules in CC **5** were removed by SQUEEZE option in PLATON.[25] Details of the crystal structures, data collection and refinement are summarized in Table 2.

Table 2. Crystallographic data and structure refinement for CCs **1**-**5**.

	1	2	3	4	5
Formula	$C_{107}H_{114}Eu_7N_7O_{38}$	$C_{107}H_{114}Gd_7N_7O_{38}$	$C_{107}H_{114}N_7O_{38}Tb_7$	$C_{107}H_{114}Dy_7N_7O_{38}$	$C_{105}H_{111}Ho_7N_6O_{38}$
M_r (g mol^{-1})	3169.77	3206.80	3218.49	3243.55	3219.51

Crystal system	Triclinic	Triclinic	Triclinic	Triclinic	Triclinic
Space group	*P*-1	*P*-1	*P*-1	*P*-1	*P*-1
T (K)	173(2)	173(2)	173(2)	172(2)	173(2)
a (Å)	18.0130(6)	18.0183(8)	17.9702(7)	17.9822(7)	17.9776(9)
b (Å)	20.1969(7)	20.0297(9)	20.0336(8)	19.9950(7)	19.8769(10)
c (Å)	20.4142(8)	20.3905(10)	20.3553(9)	20.2914(7)	20.2882(10)
α (°)	61.9780(10)	62.2680(10)	62.2610(10)	62.4550(10)	62.6010(10)
β (°)	66.6930(10)	66.8790(10)	66.9110(10)	66.9710(10)	66.9410(10)
γ (°)	76.8880(10)	77.0100(10)	76.9230(10)	77.0790(10)	77.222(2)
V (Å^3)	6013.5(4)	5982.5(5)	5957.8(4)	5945.2(4)	5914.8(5)
Z	2	2	2	2	2
D_c (g cm^{-3})	1.751	1.780	1.794	1.812	1.808
μ (mm^{-1})	3.674	3.904	4.179	4.423	4.704
F(000)	3100	3114	3128	3142	3112
Reflns collected	48508	58772	58943	58258	58853
Unique reflns	21886	21721	21698	21586	21536
R_{int}	0.0587	0.1084	0.0682	0.0745	0.1040
GOF	1.022	0.954	1.005	1.008	1.024
R_1(I > 2σ)	0.0495	0.0480	0.0539	0.0441	0.0703
wR_2 (all data)	0.1097	0.1136	0.1534	0.1096	0.2241
Max. diff. peak / hole (e Å^{-3})	3.939/ -1.250	2.533/-1.697	4.023/ -1.815	2.710/ -1.429	4.972/ -2.643
CCDC	1526731	1526732	1526733	1526734	1526735

Acknowledgements

This work was supported by the National Natural Science Foundation of China (21501093) and the Natural Science Foundation of Jiangsu Province (BK20150768).

Keywords: Lanthanide • Coordination cluster • Diethylene glycol • Magnetic relaxation • Magnetocaloric effect

[1] a) D. N. Woodruff, R. E. P. Winpenny, R. A. Layfield, *Chem. Rev*. **2013**, *113*, 5110; b) P. Zhang, Y. N. Guo, J. Tang, *Coord. Chem. Rev*. **2013**, *257*, 1728; c) R. Sessoli, A. K. Powell, *Coord. Chem. Rev*. **2009**, *253*, 2328.

[2] a) J. L. Liu, Y. C. Chen, F. S. Guo, M. L. Tong, *Coord. Chem. Rev*. **2014**, *281*, 26; b) Y. Z. Zheng, G. J. Zhou, Z. Zheng, R. E. P. Winpenny, *Chem. Soc. Rev*. **2014**, *43*, 1462; c) Y. C. Chen, J. L. Liu, M. L. Tong, *Struct. Bond* **2017,** *173*, 189.

[3] a) J. C. G. Bünzli, *Coord. Chem. Rev*. **2015**, *293-294*, 19; b)X. Yang, S. Wang, C. Wang, S. Huang, R. A. Jones, *Struct. Bond* **2017**, *173*, 155; c) F. L. Natur, G. Calvez, J. P. Guégan, L. L. Pollès, X. Trivelli, K. Bernot, C. Daiguebonne, C. Neaime, K. Costuas, F. Grasset, O. Guillou, *Inorg. Chem*. **2015**, *54*, 6043.

[4] a) F. Troiania, M. Affronte, *Chem. Soc. Rev*. **2011**, *40*, 3119; b) M. Affronte, *J. Mater. Chem*. **2009**, *19*, 1731; c) L. Bogani, W. Wernsdorfer, *Nat. Mater*. **2008**, *7*, 179; d) M. N. Leuenberger, D. Loss, *Nature* **2001**, *414*, 789.

[5] a) S. V. Eliseeva, J. C. G. Bünzli, *Chem. Soc. Rev*. **2010**, *39*, 189; b) P. H. Guo, J. L. Liu, J. H. Jia, J. Wang, F. S. Guo, Y. C. Chen, W. Q. Lin, J. D. Leng, D. H. Bao, X. D. Zhang, J. H. Luo, M. L. Tong, *Chem. Eur. J*. **2013**, *19*, 8769.

[6] a) S. Das, A. Dey, S. Kundu, S. Biswas, R. S. Narayanan, S. Titos-Padilla, G. Lorusso, M. Evangelisti, E. Colacio, V. Chandrasekhar, *Chem. Eur. J*. **2015**, *21*, 16955; b) F. Luan, T. Liu, P. Yan, X. Zou, Y. Li, G. Li, *Inorg. Chem*. **2015**, *54*, 3485; c) H. Ke, G. F. Xu, L. Zhao, J. Tang X. Y. Zhang, H. J. Zhang, *Chem. Eur. J*. **2009**, *15*, 10335.

[7] a) P. C. Andrews, W. J. Gee, P. C. Junk, M. Massi, *New J. Chem*. **2013**, *37*, 35; b) A. T. Wagner, P. W. Roesky, *Eur. J. Inorg. Chem*. **2016**, 782.

[8] a) Y. X. Ren, X. J. Zheng, L. C. Li, D. Q. Yuan, M. An, L. P. Jin, *Inorg. Chem*. **2014**, *53*, 12234; b) X. Gu, D. Xue, *Inorg. Chem*. **2007**, *46*, 3212 c) Y. Miao, J. L. Liu, J. D. Leng, Z. J. Lin, M. L. Tong, *CrystEngComm* **2011**, *13*, 3345; d) L. Huang, L. Han, W. Feng, L. Zheng, Z. Zhang, Y. Xu, Q. Chen, D. Zhu, S. Niu, *Cryst. Growth Des*. **2010**, *10*, 2548.

[9] a) G. Abbas, Y. Lan, G. E. Kostakis, W. Wernsdorfer, C. E. Anson, A. K. Powell, *Inorg. Chem*. **2010**, *49*, 8067; b) Y. X. Wang, W. Shi, H. Li, Y. Song, L. Fang, Y. Lan, A. K. Powell, W. Wernsdorfer, L. Ungur, L. F. Chibotaru, M. Shen, P. Cheng, *Chem. Sci*. **2012**, *3*, 3366; c) S. K. Langley, B. Moubaraki, C. M. Forsyth, I. A. Gass, K. S. Murray, *Dalton Trans*. **2010**, *39*, 1705.

[10] a) Y. Bi, X. T. Wang, W. Liao, X. Wang, R. Deng, H. Zhang, S. Gao, *Inorg. Chem*. **2009**, *48*, 11743; b) C. M. Liu, D. Q. Zhang, X. Hao, D. B. Zhu, *Cryst. Growth Des*. **2012**, *12*, 2948; c) R. E. Fairbairn, R. McLellan R. D. McIntosh, S. M. Taylor, E. K. Brechin, S. J. Dalgarno, *Chem. Commun*. **2012**, *48*, 8493; d) D. D' Alessio, A. N. Sobolev, B. W. Skelton, R. O. Fuller, R. C. Woodward, N. A. Lengkeek, B. H. Fraser, M Massi, M. I. Ogden, *J. Am. Chem. Soc*. **2014**, *136*, 15122.

[11] a) A. S. R. Chesman, D. R. Turner, B. Moubaraki, K. S. Murray, G. B. Deacon, S. R. Batten, *Dalton Trans*. **2012**, *41*, 10903; b) X. L. Li, L. F. He, X. L. Feng, Y. Song, M. Hu, L. F. Han, X. J. Zheng, Z. H. Zhang, S. M. Fang, *CrystEngComm* **2011**, *13*, 3643; c) D. T. Thielemann, A. T. Wagner, Y. Lan, P. Ona-Burgos, I. Fernádez, E. S. Rösch, D. K. Kölmel, A. K. Powell, S. Bräse, P. W. Roesky, *Chem. Eur. J*. **2015**, *21*, 2813; d) Y. Y. Zhou, B. Geng, Z. W. Zhang, Q. Guan, J. L. Lu, Q. B. Bo, *Inorg. Chem*. **2016**, *55*, 2037; e) K. Wang, Z. L. Chen, H. H. Zou, K. Hu, H. Y. Li, Z. Zhang, W. Y. Sun, F. P. Liang, *Chem. Commun*. **2016**, *52*, 8297; f) W. Q. Lin, X. F. Liao, J. H. Jia, J. D. Leng, J. L. Liu, F. S. Guo, M. L.

Tong, *Chem. Eur. J.* **2013**, *19*, 12254; g) I. L. Malaestean, A. Ellern, S. Baca, P. Kögerler, *Chem. Commun*. **2012**, *48*, 1449; h) L. X. Chang, G. Xiong, L. Wang, P. Cheng, B. Zhao, *Chem. Commun*. **2013**, *49*, 1055; i) Y. Zhang, L. Huang, H. Miao, H. X. Wan, H. Mei, Y. Liu, Y. Xu, *Chem. Eur. J.* **2015**, *21*, 3234; j) X. Y. Zheng, J. B. Peng, X. J. Kong, L. S. Long, L. S. Zheng, *Inorg. Chem. Front.* **2016**, *3*, 320; k) M. Romanelli, G. A. Kumar, T. J. Emge, R. E. Riman, J. G. Brennan, *Angew. Chem. Int. Ed.* **2008**, *47*, 6049; l) M. Wu, F. Jiang, X. Kong, D. Yuan, L. Long, S. A. Al-Thabaitic, M. Hong, *Chem. Sci*. **2013**, *4*, 3104; m) F. S. Guo, Y. C. Chen, L. L. Mao, W. Q. Lin, J. D. Leng, R. Tarasenko, M. Orendáč, J. Prokleška, V. Sechovský, M. L. Tong, *Chem. Eur. J.* **2013**, *19*, 14876; n) L. Chen, J. Y. Guo, X. Xu, W. W. Ju, D. Zhang, D. R. Zhu, Y. Xu, *Chem. Commun*. **2013**, *49*, 9728; o) J. Dong, P. Cui, P. F. Shi, P. Cheng, B. Zhao, *J. Am. Chem. Soc*. **2015**, *137*, 15988; p) X. J. Kong, Y. Wu, L. S. Long, L. S. Zheng, Z. Zheng, *J. Am. Chem. Soc*. **2009**, *131*, 6918; q) L. Qin, Y. Z. Yu, P. Q. Liao, W. Xue, Z. Zheng, X. M. Chen, Y. Z. Zheng, *Adv. Mater.* **2016**, *28*, 10772; r) J. B. Peng, X. J. Kong, Q. C. Zhang, M. Orendáč, J. Prokleška, Y. P. Ren, L. S. Long, Z. Zheng, L. S. Zheng, *J. Am. Chem. Soc*. **2014**, *136*, 17938.

[12] a) J. W. Sharples, Y. Z. Zheng, F. Tuna, E. J. McInnes, D. Collison, *Chem. Commun*. **2011**, *47*, 7650; b) E. M. Pineda, G. Lorusso, K. H. Zangana, E. Palacios, J. Schnack, M. Evangelisti, R. E. P. Winpenny, E. J. L. McInnes, *Chem. Sci*. **2016**, *7*, 4891; c) E. C. Mazarakioti, K. M. Poole, L. Cunha-Silva, G. Christou, T. C. Stamatatos, *Dalton Trans*. **2014**, *43*, 11456; d) W. H. Fang, L. Cheng, L. Huang, G. Y. Yang, *Inorg. Chem*. **2013**, *52*, 6; e) S. M. Taylor, S. Sanz, R. D. McIntosh, C. M. Beavers, S. J. Teat, E. K. Brechin, S. J. Dalgarno, *Chem. Eur. J.* **2012**, *18*, 16014; f) A. B. Canaj, G. K. Tsikalas, A. Philippidis, A. Spyros, C. J. Milios, *Dalton Trans*. **2014**, *43*, 12486; g) J. Goura, J. P. S. Walsh, F. Tuna, V. Chandrasekhar, *Dalton Trans*. **2015**, *44*, 1142; h) F. L. Hu, F. L. Jiang, J. Zheng, M. Y. Wu, J. D. Pang, M. C. Hong, *Inorg. Chem*. **2015**, *54*, 6081; i) X. J. Zheng, L. P. Jin, S. Gao, *Inorg. Chem*. **2004**, *43*, 1600; j) H. Tian, S. S. Bao, L. M. Zheng, *Chem. Commun*. **2016**, *52*, 2314; k) H. Tian, S. S. Bao, L. M. Zheng, *Eur. J. Inorg. Chem.* **2016**, 3184; l) E. C. Mazarakioti, L. Cunha-Silva, V. Bekiari, A. Escuer, T. C. Stamatatos, *RSC Adv*. **2015**, *5*, 92534; m) F. S. Guo, P. H. Guo, Z. S. Meng, M. L. Tong, *Polyhedron* **2011**, *30*, 3079.

[13] a) J. A. Teprovich Junior, M. N. Balili, T. Pintauer, R. A. Flowers II, *Angew. Chem., Int. Ed. Engl*. **2007**, *46*, 8160; b) H. L. Keller, D. Gruner, T. Oldag, *Z. Krist-New Cryst. St*. **2009**, *224*, 31; c) J. Gu, X. Hu, Q. Li, L. Chen, *Chinese J. Inorg. Chem*. **1998**, *14*, 313; d) H. Naruke, T. Yamase, H. Ohno, *J. Alloy Compd*. **1997**, *261*, 140.

[14] a) S. Y. Lin, L. Zhao, H. Ke, Y. N. Guo, J. Tang, Y. Guo, J. Dou, *Dalton Trans*. **2012**, *41*, 3248; b) M. L. Reddy, S. Sivakumar, *Dalton Trans*. **2013**, *42*, 2663.

[15] a) M. Pinsky, D. Avnir, *Inorg. Chem.* **1998**, *37*, 5575; b) D. Casanova, J. Cirera, M. Llunell, P. Alemany, D. Avnir, S. Alvarez, *J. Am. Chem. Soc*. **2004**, *126*, 1755; c) J. Cirera, E. Ruiz, S. Alvarez, *Chem. Eur. J.* **2006**, *12*, 3162.

[16] G. E. Kostakis, V. A. Blatov, D. M. Proserpio, *Dalton Trans*. **2012**, *41*, 4634.

[17] G. Novitchi, G. Pilet, L. Ungur, V. V. Moshchalkov, W. Wernsdorfer, L. F Chibotaru, D. Luneau, A. K. Powell, *Chem. Sci*. **2012**, *3*, 1169.

[18] J. Bartolomé, G. Filoti, V. Kuncser, G. Schinteie, V. Mereacre, C. E. Anson, A. K. Powell, D. Prodius, C. Turta, *Phys. Rev. B* **2009**, *80*, 014430.

[19] a) R. J. Blagg, F. Tuna, E. J. L. McInnes, R. E. P. Winpenny, *Chem. Commun*. **2011**, *47*, 10587; b) H. K. Zangana, E. M. Pineda, J. Schnack R. E. P. Winpenny, *Dalton Trans*. **2013**, *42*, 14045; c) S. J. Liu, J. P. Zhao, J. Tao, J. M. Jia, S. D. Han, Y. Li, Y. C. Chen, X. H. Bu, *Inorg. Chem*. **2013**, *52*, 9163; d) Y. Zheng, Q. C. Zhang, L. S. Long, R. B. Huang, A. Müller, J. Schnack, L. S. Zheng, Z. Zheng, *Chem. Commun*. **2013**, *49*, 36.

[20] F. S. Richardson, *Chem. Rev*. **1982**, *82*, 541.

[21] H. Nakai, J. Seo, K. Kitagawa, T. Goto, T. Matsumoto, S. Ogo, *Dalton Trans*. **2016**, *45*, 9492.

[22] W. Chu, Q. Sun, X. Yao, P. Yan, G. An, G. Li, *RSC Adv*. **2015**, *5*, 94802

[23] C. M. Liu, D. Q. Zhang, Y. S. Zhao, X. Hao, D. B. Zhu, *Inorg. Chem. Front*. **2016**, *3*, 1076.

[24] G. M. Sheldrick, *Acta Cryst.* **2008**, *A64*, 112.

[25] A. L. Spek, *J. Appl. Crystallogr*. **2003**, *36*, 7.

10.1002/ejic.201700168

WILEY-VCH

Entry for the Table of Contents (Please choose one layout)

FULL PAPER

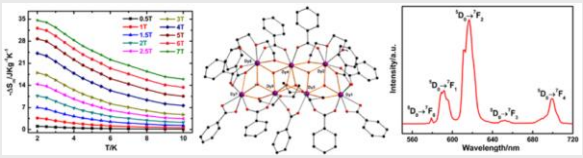

Five heptanuclear lanthanide coordination clusters with scarce tip-sharing double-butterfly topology have been isolated, and their single molecule magnet, magnetic cooler and emission behaviors are presented.

Coordination Cluster

Guo Peng,[a] Ying-Ying Zhang,[a] Zhao-Yang Li[b] and George E. Kostakis[c]*

Page No. – Page No.

First examples of polynuclear lanthanide diethylene glycol based coordination clusters